

Computational assessment of subcritical and delayed onset in spiral Poiseuille flow experiments

By DAVID L. COTRELL[†], SARMA L. RANI[‡]
AND ARNE J. PEARLSTEIN[¶]

Department of Mechanical and Industrial Engineering, University of Illinois at Urbana-Champaign,
1206 West Green Street, Urbana, IL 61801, USA

(Received 29 April 2003 and in revised form 30 January 2004)

For spiral Poiseuille flow with radius ratios $\eta \equiv R_i/R_o = 0.77$ and 0.95 , we have computed complete linear stability boundaries, where R_i and R_o are the inner and outer cylinder radii, respectively. The analysis accounts for arbitrary disturbances of infinitesimal amplitude over the entire range of Reynolds numbers Re for which the flow is stable for some range of Taylor number Ta , and extends previous work to several non-zero rotation rate ratios $\mu \equiv \Omega_o/\Omega_i$, where Ω_i and Ω_o are the (signed) angular speeds. For each combination of μ and η , there is a wide range of Re for which the critical Ta is nearly independent of Re , followed by a precipitous drop to $Ta = 0$ at the Re at which non-rotating annular Poiseuille flow becomes unstable with respect to a Tollmien–Schlichting-like disturbance. Comparison is also made to a wealth of experimental data for the onset of instability. For $Re > 0$, we compute critical values of Ta for most of the $\mu = 0$ data, and for all of the non-zero- μ data. For $\mu = 0$ and $\eta = 0.955$, agreement with data from an annulus with aspect ratio (length divided by gap) greater than 570 is within 3.2% for $Re \leq 325$ (based on the gap and mean axial speed), strongly suggesting that no finite-amplitude instability occurs over this range of Re . At higher Re , onset is delayed, with experimental values of Ta_{crit} exceeding computed values. For $\mu = 0$ and smaller η , comparison to experiment (with smaller aspect ratios) at low Re is slightly less good. For $\eta = 0.77$ and a range of μ , agreement with experiment is very good for $Re < 135$ except at the most positive or negative μ (where $Ta_{crit}^{expt} > Ta_{crit}^{comp}$), whereas for $Re \geq 166$, $Ta_{crit}^{expt} > Ta_{crit}^{comp}$ for all but the most positive μ . For $\eta = 0.9497$ and 0.959 and all but the most extreme values of μ , agreement is excellent (generally within 2%) up to the largest Re considered experimentally (200), again suggesting that finite-amplitude instability is unimportant.

1. Introduction

Cottrell & Pearlstein (2004), in a companion paper hereinafter referred to as Part 1, present complete stability boundaries for spiral Poiseuille flow (SPF) for the radius ratio $\eta \equiv R_i/R_o = 0.5$ and several rotation rate ratios $\mu \equiv \Omega_o/\Omega_i$ over the entire range of Reynolds number $Re \equiv \bar{V}_Z (R_o - R_i)/\nu$ for which the flow is linearly stable at any Taylor number $Ta \equiv \Omega_i (R_o - R_i)^2/\nu$, where ν and \bar{V}_Z are the kinematic viscosity and

[†] Present address: NIST, 100 Bureau Drive, Gaithersburg, MD 20899-8910, USA.

[‡] Present address: Department of Mechanical and Aerospace Engineering, Cornell University, Ithaca, NY 14853, USA.

[¶] Author to whom correspondence should be addressed: ajp@uiuc.edu

the mean of the axial component of the base-flow velocity, and Ω_i and Ω_o are the (signed) angular velocities of the inner and outer cylinders, whose radii are R_i and R_o , respectively. Their work, for the η values in the experiments and computations of Takeuchi & Jankowski (1981) and computations of Meseguer & Marques (2002), extends the Re range investigated eightyfold, and shows how the $Re = 0$ centrifugal instability connects to a high- Re Tollmien–Schlichting (TS)-like instability. The results of Part 1 also establish that when μ exceeds the Rayleigh limit $\mu = \eta^2$, there is an Re range in which SPF is linearly stable for all Ta , and that when $\mu \neq 1$, there is a range in which two critical Ta values exist for each Re .

Contemporaneous to the work of Takeuchi & Jankowski, Ng & Turner (1982) reported computations for $\mu = 0$, considering arbitrary infinitesimal disturbances over $0 \leq Re \leq 6000$ for $\eta = 0.77$ and 0.95 , and axisymmetric disturbances up to $Re = 7739.5$ for $\eta = 0.95$. For both radius ratios, the critical Taylor number, Ta_{crit} , increases with Re before reaching a broad plateau. For $\eta = 0.95$, the Ta at which SPF becomes unstable with respect to axisymmetric disturbances was shown to decrease rapidly beyond $Re = 6000$. Their results agree well with the $\mu = 0$ data of Mavec (1973) up to $Re = 400$ for $\eta = 0.77$, and Snyder (1962, 1965) up to $Re = 200$ for $\eta \approx 0.95$.

Here, for the radius ratios of Ng & Turner, which are equal or close to those for most of the experimental work, we compute complete stability boundaries at several μ , including the $\mu = 0$ cases studied by Ng & Turner. For $Re > 0$, we also present results for most of the combinations of Re and η for the $\mu = 0$ data (Kaye & Elgar 1958; Becker & Kaye 1962; Sorour 1977; Gravas & Martin 1978; Sorour & Coney 1979; Greaves, Grosvenor & Martin 1983), and all combinations of Re and η for $\mu \neq 0$ (Snyder 1965; Mavec 1973).

The stability boundaries extend the earlier work of Ng & Turner for $\eta = 0.77$ and 0.95 by accounting for arbitrary disturbances of infinitesimal amplitude over the full Re range of the linear stability boundary. We show that in the only SPF case ($\mu = 0$, $\eta = 0.95$) for which a connection of the $Re = 0$ centrifugal instability to the high- Re shear instability had been made (Ng & Turner 1982), transition occurs from a non-axisymmetric centrifugal instability to a non-axisymmetric TS-like instability, at an Re in the range where Ng & Turner considered only axisymmetric disturbances.

Takeuchi & Jankowski and Ng & Turner noted that beyond some μ -dependent Re value, experimental Ta_{crit} values found by flow visualization lie above critical values computed by linear stability theory, to an extent that increases with Re . Takeuchi & Jankowski concluded that “the linear theory has an even greater range of applicability than demonstrated here,” and proposed two mechanisms for systematic underprediction of Ta_{crit} (or ‘delayed onset’) at higher Re . The first is associated with experimental annuli insufficiently long to allow secondary flow to develop to detectable amplitudes. The second pertains to experiments in which $dTa_{crit}/dRe < 0$ using a constant-head pump, in which case formation of weak vortical structures would have the effect of reducing the mean axial velocity. ‘Delayed onset’ might also be associated with instability of an incompletely developed ‘base flow’, due to entrance effects. We use ‘subcritical onset’ to refer to onset below the critical Ta due to any reason, including ‘finite-amplitude’ disturbances having an amplitude threshold, as well as instability associated with an incompletely developed base flow at a Ta below that predicted for the fully developed base flow.

Comparison to experimental data allows us to draw some conclusions about the range of Re , μ , and η for which linear stability analysis is valid, and about the effects of annulus aspect ratio $L/(R_o - R_i)$ on the apparent critical Ta , where L is the annulus length.

Essentially perfect agreement between our results and the $\mu=0$ data of Sorour & Coney at $\eta=0.955$ and the $\mu=0$ and $\mu \neq 0$ data of Mavec (1973) at $\eta=0.77$ and Snyder (1965) at $\eta \approx 0.95$ shows that over a broad range of Re , μ , and η , finite-amplitude instability does not occur, and that onset delay mechanisms are also unimportant. Thus, for at least some combinations of μ and η , it is likely that instability sets in through infinitesimal disturbances up to Re in excess of several hundred. The results also allow us to identify regimes in which either subcritical or delayed onset occurs.

Numerical methods were discussed in Part 1. The remainder of the present paper is organized as follows. In §2, complete stability boundaries for SPF are presented for $\eta=0.77$ and 0.95 and several values of μ . In §3, we present results for specific experimental combinations of Re , μ , and η , for which no previous comparison to theory has been made, along with detailed comparison to data and discussion of implications for interpretation of data. Additional discussion follows in §4, and some conclusions are presented in §5.

2. Complete stability boundaries

For the radius ratios η (0.77 and 0.95) considered by Ng & Turner, we report complete linear stability boundaries in the (Re, Ta) -plane at several values of the rotation rate ratio μ , accounting for arbitrary three-dimensional disturbances of infinitesimal amplitude. Convergence tests, described in Part I for $\eta=0.5$, were performed for $\eta=0.77$ and 0.95 at each μ . In general, the number of radial expansion functions required for convergence decreases with increasing η . Except where otherwise indicated, our results are in excellent agreement with those tabulated by Ng & Turner over the Re ranges they investigated. Our results cover the entire range of Re for which SPF is linearly stable, from $Re=0$ (the circular Couette limit) to Re_{AP} (beyond which SPF is unstable for all Ta , corresponding to onset of TS-like instability in non-rotating annular Poiseuille flow). We note that Re_{AP} is independent of μ , since it corresponds to the non-rotating limit.

2.1. Stability boundary for $\eta=0.77$

For $\mu=0$ and $\eta=0.77$, Ng & Turner accounted for axisymmetric and non-axisymmetric disturbances up to $Re=6000$. As discussed in §3 of Part 1 in the context of code validation, comparison to their results shows excellent agreement over that range. At higher Re , figure 1(a) shows that Ta_{crit} continues on a plateau ($Ta_{crit}=58.6$) until the transition at $Re^*=8677$, and falls rapidly to zero over the range $Re^* < Re \leq Re_{AP}=8883.3$. The value of Re_{AP} is in good agreement with previous graphical results (Mahadevan & Lilley 1977; Garg 1980) for the stability of nonrotating annular Poiseuille flow.

There are qualitative as well as quantitative differences between the $\eta=0.5$ and 0.77 cases. For $\eta=0.77$, figure 1(a) shows that Ta_{crit} increases with Re up to $Re \approx 200$. The stabilization by axial flow over the entire range of centrifugal instability contrasts with the $\eta=0.5$ case, where increasing Re stabilized and destabilized SPF in different parts of the pre-plateau range $10 < Re < 400$. For $\eta=0.77$, Ta_{crit} is nearly constant in a plateau range ($200 < Re < 8000$) that starts at smaller Re than for $\eta=0.5$. The value of Re_{AP} (8883.3) is also smaller than that (10 359) for $\eta=0.5$. The dependence of Re_{AP} on η is part of a systematic variation from $Re_{AP}=5772$ as $\eta \rightarrow 1$ (see §4.1) to $Re_{AP} \rightarrow \infty$ as $\eta \rightarrow \hat{\eta}$ from above, where $\hat{\eta} < 0.15$ is the minimum η for which annular Poiseuille flow is unstable (Mahadevan & Lilley 1977; Garg 1980).

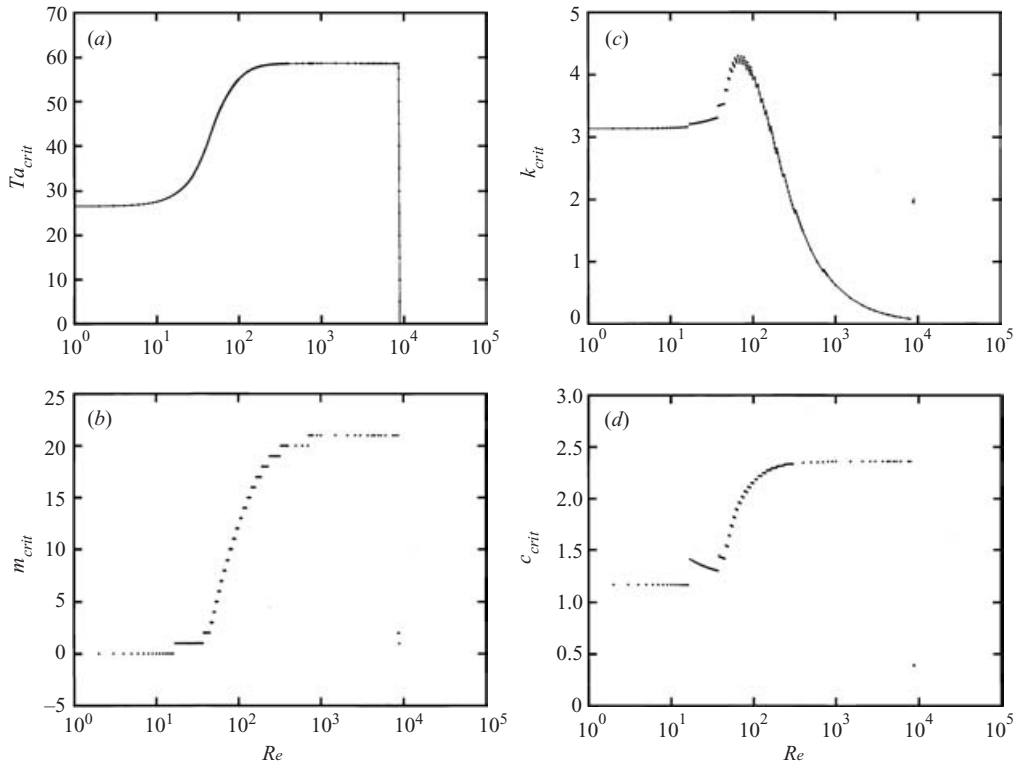


FIGURE 1. For $\mu = 0$ and $\eta = 0.77$: (a) critical Ta , (b) critical m , (c) critical k , (d) critical c versus Re .

As for $\eta = 0.5$, figure 1(b) shows that m_{crit} increases over $0 \leq Re \leq Re^*$ by unit steps. Our results agree with tabulated values of Ng & Turner except at $Re = 300$ and 500 where, as discussed in Part 1, we find critical azimuthal wavenumbers $m_{crit} = 19$ and 20 , respectively, in contrast to their values of 20 and 21 , apparently due to our tighter control of convergence. Figure 1(b) shows that $m_{crit} = 21$ over much of the high- Re plateau, compared to a maximum $m_{crit} = 7$ for $\eta = 0.5$. As Re passes through Re^* , m_{crit} decreases abruptly from 21 to 2 . On the TS-like branch, m_{crit} suffers a final step decrease to 1 , its value at Re_{AP} . This contrasts to the constant $m_{crit} = 2$ on the TS-like branch for $\eta = 0.5$.

As for $\eta = 0.5$, figures 1(b) and 1(c) show that the discontinuities of the critical axial wavenumber k_{crit} occur at Re values at which m_{crit} jumps, as described by Ng & Turner. There is again an Re (≈ 42) below which k_{crit} increases monotonically with Re for each m_{crit} , and above which k_{crit} decreases monotonically with Re for each m_{crit} . We note that k_{crit} again decreases as Re approaches Re^* from below, as found for $\eta = 0.5$.

For $\eta = 0.77$, figure 1(d) shows the piecewise-continuous Re dependence of the critical wave speed c_{crit} . Our computed c_{crit} values are in excellent agreement with those tabulated by Ng & Turner (1982) at their 18 Re values in the range $0.01 \leq Re \leq 6000$, except at $Re = 300$ and 500 , where our m_{crit} values differ from theirs by 1 . As for $\eta = 0.5$, the almost constant c_{crit} when $m_{crit} = 0$ corresponds to a dimensional frequency increasing nearly linearly from zero as \bar{V}_Z increases. For each $m_{crit} < 15$, c_{crit} decreases monotonically with Re , while for $m_{crit} \geq 15$, c_{crit} increases piecewise continuously up to

$m_{crit} = 21$. This contrasts with the $\eta = 0.5$ results, where c_{crit} decreased monotonically with Re for each m_{crit} . For $800 < Re \leq Re^*$ ($m_{crit} = 21$), c_{crit} remains nearly constant ($c_{crit} \approx 2.36$). As Re passes through Re^* , c_{crit} decreases abruptly to about 0.39, and then decreases slightly to its $Ta = 0$ value of 0.38 as Re increases from Re^* to Re_{AP} .

The stair-step behaviour of m_{crit} and the associated discontinuous dependence of k_{crit} and c_{crit} on Re indicate that Ta_{crit} is a continuous but only piecewise-differentiable function of Re . That the slope discontinuities are less apparent than for $\eta = 0.5$ reflects the fact that the values of m_{crit} are considerably larger for $\eta = 0.77$, so that $(m + 1)/m$ and $(m + 1)^2/m^2$, the ratios of consecutive m -dependent terms in the disturbance equations, are closer to unity at the larger η . The step ‘width’ (i.e. the Re range for which m_{crit} is constant) is considerably smaller for $\eta = 0.77$ than for $\eta = 0.5$, corresponding to the larger range of critical m for $\eta = 0.77$ ($0 \leq m_{crit} \leq 21$) than for $\eta = 0.5$ ($0 \leq m_{crit} \leq 7$).

For $\mu = 0.2$ and $\eta = 0.77$, figure 2(a) shows that Ta_{crit} increases monotonically with Re from 28.90 at $Re = 0$, nearly doubling to a maximum of 56.78 near $Re = 115$, and decreases slightly to a plateau value of about 55.6 for Re up to Re^* . The critical m (not shown) increases to 20 in unit steps for $0 \leq Re \leq 900$, and remains constant for $900 \leq Re < Re^* = 8712$. As one passes through Re^* , m_{crit} jumps from 20 to 2. As Ta decreases below about 10, m_{crit} on the nearly vertical TS-like branch again decreases from 2 to 1, the value it maintains all the way to $Re_{AP} = 8883.3$, where $Ta_{crit} = 0$.

The critical k (also not shown) increases piecewise continuously with Re until reaching a global maximum near $Re = 60$, beyond which it decreases sharply until Re^* . The Re variation of k_{crit} is similar to that found for $\eta = 0.5$ and $\mu = 0.2$. The dependence of c_{crit} on Re is very similar to that for $\mu = 0$.

For $\mu = -0.5$, the $\eta = 0.5$ and 0.77 stability boundaries differ significantly. First, figure 2(b) shows that for $\eta = 0.77$, SPF is stabilized as Re increases, with Ta_{crit} increasing monotonically from its $Re = 0$ value of 32.83 to about 69 on a broad plateau between about $Re = 700$ and the drop at $Re^* = 8579$. This contrasts with the $\eta = 0.5$ case, where SPF is alternately destabilized and stabilized for $0 < Re < 1000$. Second, for $\eta = 0.77$, the nearly constant Ta_{crit} on the plateau (≈ 69) is greater than the $Re = 0$ value, unlike the $\eta = 0.5$ case, for which Ta_{crit} on the plateau lies below the $Re = 0$ value. Finally, the scalloped behaviour for $\eta = 0.77$ is less pronounced than for $\eta = 0.5$.

As for $\eta = 0.5$, the computed m_{crit} (not shown) increases in unit steps for $Re < Re^*$, with $m_{crit} = 0$ up to $Re \approx 4$, and onset through non-axisymmetric disturbances (m_{crit} up to 24) at higher Re . We compute $m_{crit} = 23$ and 24 over relatively wide ranges on the high- Re plateau. As Re passes through Re^* , m_{crit} jumps from 24 to 2. For $Re^* < Re < Re_{AP}$, m_{crit} again decreases from 2 to 1. The piecewise-continuous dependence of k_{crit} and c_{crit} on Re is qualitatively similar to that for $\eta = 0.5$.

2.2. Stability boundaries for $\eta = 0.95$

For $\eta = 0.95$ and $\mu = 0$, Ng & Turner computed Ta_{crit} for $0 \leq Re \leq 6000$, and the Ta at which SPF would be destabilized by axisymmetric disturbances for $6000 \leq Re \leq 7739.5$. We have shown that Re_{AP} is indeed 7739.5 (where $m_{crit} = 0$), and completed the stability boundary by considering non-axisymmetric disturbances up to that Re . Comparison to the results of Ng & Turner over $0 \leq Re \leq 6000$ (see Part 1) is excellent. For $Re > 6000$, our results agree with theirs only in a very narrow range just below $Re_{AP} = 7739.5$, in which m_{crit} is actually zero. In particular, at $Re = 7000$, Ng & Turner report a Taylor number for the onset of axisymmetric

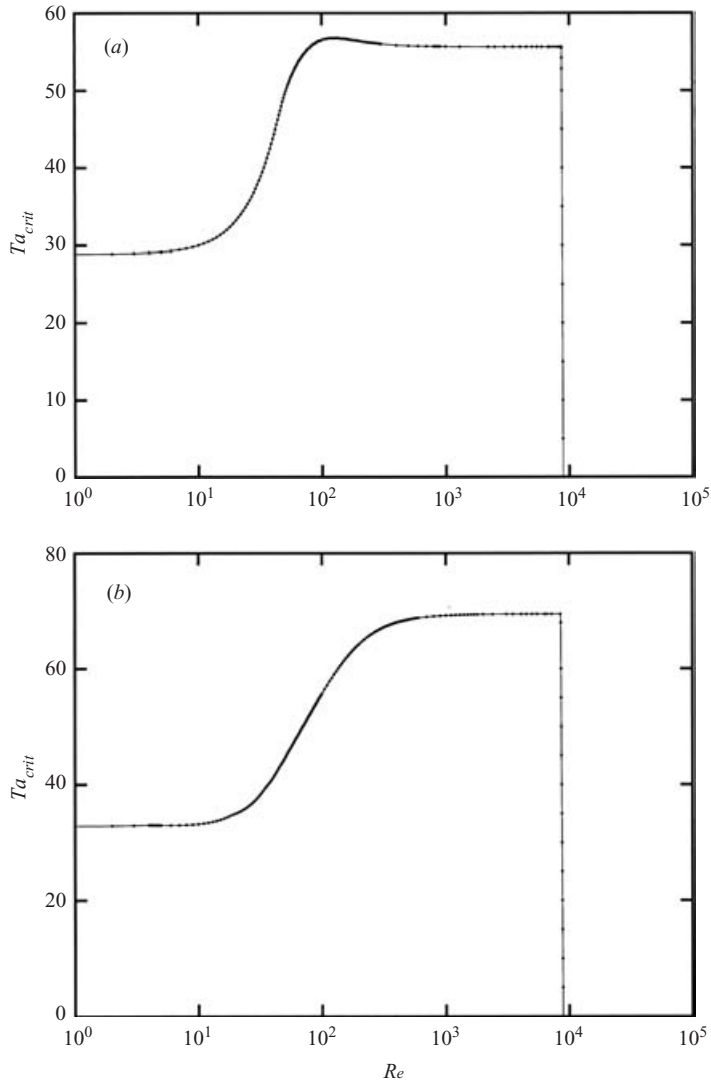


FIGURE 2. Critical Ta versus Re for $\eta = 0.77$: (a) $\mu = 0.2$, (b) $\mu = -0.5$.

instability which, using the present scaling, corresponds to $Ta = 367.68$, as opposed to our value of 47.56 (for $m_{crit} = 149$).

For $\eta = 0.95$, the stability boundary (figure 3) is qualitatively similar to that for $\eta = 0.77$, with the nearly constant Ta_{crit} (≈ 47) on the high- Re plateau ($1000 < Re < 7716$) being greater than at $Re = 0$. For $\eta = 0.95$, Ta_{crit} is smaller than for $\eta = 0.5$ and 0.77.

As for $\eta = 0.5$ and 0.77, m_{crit} (not shown) increases by unit steps (from 0 to 149) over $0 \leq Re < Re^*$. At Re^* , m_{crit} jumps from 149 to 2. For $Re^* \leq Re \leq Re_{AP}$, m_{crit} decreases from 2 to 1 to 0, its value at Re_{AP} . Transition from $m_{crit} = 1$ to 0 occurs in the range $7737.55 < Re < 7739.22$, so that $m_{crit} \neq 0$ for $6000 \leq Re \leq 7737.55$, leading to the differences between our Ta_{crit} values and those of Ng & Turner in the latter range.

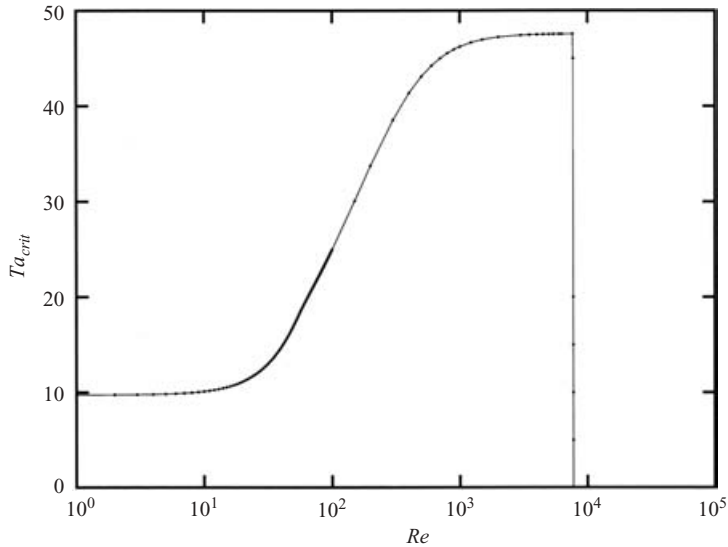


FIGURE 3. Critical Ta versus Re for $\mu = 0$ and $\eta = 0.95$.

As Re increases from zero to about 54, k_{crit} increases piecewise monotonically. Beyond $Re = 54$, k_{crit} decreases monotonically with Re over each range of constant m_{crit} . The maximum k_{crit} occurs near $Re = 120$. Again, there is excellent agreement between our m_{crit} values and those of Ng & Turner for $Re \leq 6000$. For $\eta = 0.95$, our k_{crit} and c_{crit} values are essentially identical to theirs over that range, except at $Re = 10$, 100, and 2000, where differences in c_{crit} are due to unit differences in m_{crit} . The dependence of k_{crit} and c_{crit} on Re is qualitatively similar to that for $\eta = 0.5$ and 0.77.

As discussed for $\eta = 0.77$, the narrowness of the Re ranges over which m_{crit} is constant, as well as the size of m_{crit} , contribute to the apparent smoothness of the stability boundary over the entire range of centrifugal instability, and of the k_{crit} and c_{crit} plots at high Re . For $\eta = 0.95$, the constant- m_{crit} ranges of Re are so narrow, and m_{crit} is so large, that discontinuities in k_{crit} and c_{crit} are not graphically apparent beyond about $Re = 80$ (corresponding to $m_{crit} \approx 25$). This is a consequence of the fact that for the centrifugal instability, m_{crit} grows rapidly as $\eta \rightarrow 1$ and behaves much like a continuous wavenumber. We also note that the m_{crit} values are fully resolved. Inadequate resolution (particularly use of insufficiently small tolerances for the wavenumber and Ta iterations) can lead to spurious non-monotonic variation in the computed m_{crit} values, since the minima of neutral curves for large m occur at extremely similar Ta .

3. Comparison to experiment

For $\mu = -0.5$, 0, and 0.2, Takeuchi & Jankowski compared their computed and experimental results at $\eta = 0.5$ over $0 \leq Re \leq 100$. For $\mu = 0$, Ng & Turner compared their computations at $\eta = 0.77$ to data of Nagib (1972) and Mavec (1973) up to $Re = 400$ at the same η , and computations at $\eta = 0.95$ to $\eta = 0.959$ data of Snyder (1962, 1965) up to $Re = 200$. These comparisons showed generally good agreement for small Re .

Authors	η	Re	Ta_{crit}^{expt}	Ta_{crit}^{comp}
Kaye & Elgar (1958) $L/(R_o - R_i) = 114$	0.734	0	(53.5) 29.6	30.27
		30.91	(85.1) 47.1	39.70
		47.27	(102) 56.6	49.09
		76.36	(112) 61.9	57.49
		115.2	(114) 63.3	60.65
		142.4	(117) 64.6	61.31
		193.9	(119) 66.0	61.60
		263.6	(119) 66.0	61.61
		333.3	(125) 69.3	61.56
		401.8	(128) 71.1	61.56
		551.5	(117) 64.6	61.48
Becker & Kaye (1962) $L/(R_o - R_i) \approx 172$	0.8076	0	(1930) 20.3	22.97
		26.5	(2620) 23.6	28.48
		55	(7000) 38.6	41.05
		111	(10 900) 48.2	50.86
		157.5	(16 800) 59.8	53.43
		301.5	(16 800) 59.8	55.29
		526.5	(20 700) 66.4	55.72
		796	(21 300) 67.4	55.81

TABLE 1. Comparison of experimental and computed values of Ta_{crit} for $\mu = 0$. Parentheses denote values of differently defined Taylor numbers read from figures of other authors.

Here, we consider data for which no comparison to computation has been made, including data at higher Re and larger $|\mu|$ than considered by Takeuchi & Jankowski and Ng & Turner. Results for Re and η used in the $\mu = 0$ experiments are shown in §3.1. In §3.2, computational results are presented, and detailed comparisons are made to data, for all μ in the $Re > 0$ experiments of Mavec (1973) for $\eta = 0.77$ and Snyder (1965) for $\eta = 0.9497$ and 0.9590 . Unless identified by uppercase superscript, Reynolds and Taylor numbers of other authors are reported using our definitions.

3.1. Comparison to previous experimental work ($\mu = 0$)

Critical Taylor numbers

Kaye & Elgar (1958) studied stability of SPF using smoke visualization and hot-wire anemometry for $\eta = 0.734$ and 0.820 ($L/(R_o - R_i) = 114$ and 186 , respectively). For $Re = 0$, the critical rotation rate was said to agree with linear theory to within 1% for $\eta = 0.734$; no comparison was given for $\eta = 0.820$. In both cases, Ta_{crit} initially increased with Re , reaching a maximum between $Re = 400$ and 550 for $\eta = 0.734$, and between 350 and 400 for $\eta = 0.820$. For larger Re , Ta_{crit} decreased monotonically and nearly linearly to zero at Re values near 1000 and 900 for $\eta = 0.734$ and 0.820 , respectively. For $\eta = 0.734$, table 1 shows the 11 smallest Re values read from figure 13 of Kaye & Elgar, along with their corresponding critical Taylor numbers Ta_{crit}^{KE} (in parentheses). Also shown are values of Ta_{crit}^{comp} corresponding to each Re , and values of $Ta_{crit}^{expt} = Ta_{crit}^{KE} [2(1 + \eta)/(1 - \eta)]^{1/2}$ calculated from the reported Taylor numbers. Over the Re range shown in table 1, experimental and computed results are in generally good agreement. The difference (2%) between the experimental and computed Ta_{crit} values at $Re = 0$ is comparable to the 1% difference between the experimental critical angular velocity and ‘the theoretical value predicted by Taylor’s theory’ cited by Kaye & Elgar, and provides a measure of the reading error in Ta_{crit}^{KE} . For the larger Re shown, Ta_{crit}^{expt} values lie 4–20% above Ta_{crit}^{comp} . In the Re range where Ta_{crit}^{comp} exhibits

plateau behaviour, Ta_{crit}^{expt} increases slowly until reaching a maximum at some Re between 400 and 550, beyond which it decreases. For Re values in figure 13 of Kaye & Elgar larger than shown in table 1, Ta_{crit}^{expt} decreases to zero near $Re = 1000$, while Ta_{crit}^{comp} maintains a plateau value near 61.5, ultimately falling off rapidly to zero near $Re = 10^4$ via a TS-like instability. Implications of this comparison for interpretation of these experimental results, and similar experimental results for $\eta = 0.820$ (figure 14 of Kaye & Elgar), are discussed in §4.1.

For $\mu = 0$, Yamada (1961, 1962) obtained qualitatively similar results for $\eta = 0.971$, 0.981, and 0.987. For a number of Re values between 0 and 1100, he reported critical dimensionless rotation rates at which either the ratio of the torque coefficient to its base-flow value (Yamada 1961, figure 16) or the dimensionless axial pressure drop (Yamada 1962, figure 18) increased ‘sharply’. His results, while differing somewhat among the small-gap radius ratios considered and between the two onset diagnostics, generally showed that Ta_{crit} is a unimodal function of Re , and reaches its maximum in the range $400 \leq Re \leq 700$. Beyond the maximum, Ta_{crit} values reported for both diagnostics decreased rapidly with Re . For example, at $\eta = 0.987$, the reported Ta_{crit} decreased by about 70% between its maximum near $Re = 650$ and the largest Re for which Yamada reported results, 1100. For each η , extrapolation of the reported critical Taylor numbers to zero (i.e. the annular Poiseuille limit) gives an intercept near $Re = 1200$.

For $\mu = 0$ and $\eta \approx 0.81^\dagger$, heat transfer measurements by Becker & Kaye (1962) showed that the ratio of the Nusselt number to its base-flow value undergoes a well-defined transition at a Ta_{crit} that increases with Re over $0 \leq Re \leq 1430$. (Beyond $Re = 1430$, no clear transition is evident.) At the eight smallest Reynolds numbers they considered, our table 1 shows the Taylor numbers Ta_{crit}^{BK} (in parentheses, read from their figure 4, and thought to be accurate within one or two units in the third significant figure) at onset, $Ta_{crit}^{expt} = [2Ta_{crit}^{BK}(1 - \eta)/(1 + \eta)]^{1/2}$, and Ta_{crit}^{comp} computed from our linear analysis at the same η . (Although onset is quite distinct at $Re = 1007.5$ and 1430, Nusselt numbers before onset at these two Re differed from the nominal base-flow values by about 10% and 50%, respectively. Note also that the Taylor number used by Kaye & Elgar differs from that of Becker & Kaye, and that the Reynolds number used by Kaye and co-workers differs from ours by a factor of 2.) To calculate Ta_{crit}^{expt} from Ta_{crit}^{BK} , we used $\eta = 0.8076$, the mean of the η values corresponding to the radii and gap given by Becker & Kaye.

In general, our results agree well with those of Becker & Kaye. At the four smallest Re , the experimental Ta_{crit} values lie 6–17% below linear stability predictions, while at the next four Re , the experimental values are 11–20% higher than predicted. The latter discrepancy is consistent with inadequate axial development length for the disturbance flow in the apparatus ($L/(R_o - R_i) \approx 172$) of Becker & Kaye, identified by Takeuchi & Jankowski as an explanation for a similar discrepancy between their experimental results (with $L/(R_o - R_i) \approx 115$) and their own computations. Since $dTa_{crit}/dRe \geq 0$ (see table 1) up to $Re = Re^*$ for $\eta \geq 0.77$ (see also figures 1a and 3), the alternative constant-head mechanism proposed by Takeuchi & Jankowski is not applicable in this case.

Gravas & Martin (1978) used hot-wire anemometry to investigate onset of secondary flow at $\mu = 0$ for $\eta = 0.576$, 0.81, and 0.9 over $43 \leq Re \leq 1000$. For each η ,

[†] Based on the cylinder radii given, $\eta = 0.8097 \pm 0.0008$. Based on the reported gap between cylinders and the outer cylinder radius, $\eta = 0.8055 \pm 0.0010$.

Ta_{crit} increased monotonically with Re . Here, we compare our results for the similar radius ratios of 0.5, 0.77, and 0.95, as well as computations performed at their Re and η values.

The $\eta = 0.81$ and 0.9 results of Gravas & Martin are in general qualitative agreement with our $\eta = 0.77$ and 0.95 computations, with the experimental Ta_{crit} plateaux being less well-defined. At $\eta = 0.576$, however, there is no evidence of the plateau predicted for $\eta = 0.5$ (figure 1a of Part 1). Computations at $\eta = 0.576$ show that differences are not due to different experimental and computational radius ratios, with Ta_{crit}^{comp} decreasing monotonically with Re over the same range, consistent with results for $\eta = 0.5$, whereas Ta_{crit}^{expt} increases monotonically with Re over $70 \leq Re \leq 255$ (see figure 5 of Gravas & Martin). Some of this discrepancy might be associated with annuli of small aspect ratio $L/(R_o - R_i)$ (between 32 and 175 in the experiments of Gravas & Martin), in which vortical structures have insufficient opportunity to develop to a detectable amplitude. Significant geometric imperfection (i.e. axial and azimuthal variations of the gap), as later discussed by Greaves *et al.* (1983) might also be important.

For $\mu = 0$, Sorour (1977) and Sorour & Coney (1979) used hot-wire anemometry to determine Ta_{crit} for $\eta = 0.8$ over $26 \leq Re \leq 468$ and for $\eta = 0.955$ over $26.4 \leq Re \leq 595$. For each Re , Sorour & Coney fitted a curve to critical values of $Ta^{SC} = 2Ta^2\eta^2/(1 - \eta^2)$ at nine uniformly spaced radial locations in the annular gap. Table 2 shows in parentheses the minimum Ta^{SC} on that curve as read from either figure 1 of Sorour & Coney or similar figures of Sorour, along with values of Ta_{crit}^{expt} calculated from Ta^{SC} using the corresponding η , and computed values Ta_{crit}^{comp} . (We note that the values of m_{crit} at $\eta = 0.95$ and 0.955 differ for most Re , so that even for these very similar radius ratios, we have performed specific computations for the experimental η .) Parenthetical values of Ta^{SC} up to 10^4 are thought to be correctly read to three significant figures, while larger values are thought to be in error by no more than one or two units in the fourth significant figure.

We first consider the $\eta = 0.955$ case, for which the aspect ratio is more than four times its $\eta = 0.8$ value. As shown in table 2, our results are in excellent agreement with the data for $Re \leq 325$. The maximum difference is less than 3.2%, and the mean of the absolute value of the relative difference is 2.2%, both comparable to uncertainties in Ta_{crit}^{expt} associated with readability of experimental Taylor numbers as propagated through the relationship between Ta and Ta^{SC} . The aspect ratio in the $\eta = 0.955$ experiments exceeded 570, compared to 114 and 186 for Kaye & Elgar, 172 for Becker & Kaye, 115 for Takeuchi & Jankowski, and a range of 32–175 for Gravas & Martin. From the close agreement of our computed Ta_{crit} values with the data of Sorour & Coney, we conclude that finite-amplitude instability either did not occur in their experiments, or occurred only slightly below the critical values predicted by linear stability theory. The larger aspect ratio of Sorour & Coney apparently provided sufficient streamwise length for detectable vortical structures to develop, at least for $Re \leq 325$. As Re increases, table 2 shows that the Ta at which onset is first detected in an annulus of fixed aspect ratio continues to increase, while the linear analysis predicts a plateau value of Ta_{crit} .

For $\eta = 0.8$ and $Re \leq 320$, table 2 shows that agreement between the experiments of Sorour & Coney and computation is still good, but less close than for $\eta = 0.955$. For $\eta = 0.8$, the maximum difference and mean absolute value of the relative difference over this Re range are 13% and 6.0%, respectively, with the experimental Ta_{crit} values lying at or slightly below the computed values, except at the two lowest Re and at the highest Re . (For $Re = 36.5$, the nearly identical experimental values of Ta^{SC} at each radius seem to be anomalously high.) These results are taken as evidence that for

Authors	η	Re	Ta_{crit}^{expt}	Ta_{crit}^{comp}
Sorour & Coney (1979) $L/(R_o - R_i) = 130$	0.8	26	(3620) 31.9	29.16
		36.5	(5420) 39.0	33.80
		60	(6380) 42.4	43.78
		75	(6810) 43.8	47.29
		97	(7800) 46.8	50.55
		151	(9040) 50.4	54.08
		195	(9760) 52.4	55.12
		239	(10 420) 54.1	55.60
		281	(11 120) 55.9	55.86
		320	(12 100) 58.3	56.00
		Sorour & Coney (1979) $L/(R_o - R_i) > 570$	0.955	26.4
33.5	(3440) 12.9			12.64
42	(4670) 15.0			14.32
54	(6000) 17.0			16.91
67	(8040) 19.7			19.29
78.5	(9790) 21.7			20.97
94	(11 480) 23.5			22.97
107	(12 670) 24.7			24.49
135	(15 290) 27.2			27.34
150	(16 180) 27.9			28.68
182	(19 000) 30.3			31.15
200	(20 410) 31.4			32.36
215	(22 210) 32.7			33.27
240	(24 210) 34.2			34.64
260	(26 700) 35.9			35.62
325	(32 790) 39.8			38.19
370	(36 630) 42.0			39.55
450	(44 530) 46.3			41.37
525	(51 500) 49.9			42.60
595	(57 400) 52.6	43.46		
Greaves <i>et al.</i> (1983) $L/(R_o - R_i) \approx 310$	0.909	43.75	(10 000) 22.9	21.98
		87.5	(23 000) 34.8	31.95
		131	(31 200) 40.5	37.36
		262	(45 100) 48.7	44.52
		435.5	(48 000) 50.2	47.32
		800	(43 500) 47.8	48.71
		1010	(38 000) 44.7	48.95

TABLE 2. Comparison of experimental and computed values of Ta_{crit} for $\mu = 0$. Parentheses denote values of differently defined Taylor numbers read from figures of other authors.

$Re \leq 320$, either there is no finite-amplitude instability, or finite-amplitude instability sets in at Ta values only slightly below those predicted by linear theory. The relatively small differences between experiment and computation at the highest Re suggest that the aspect ratio ($L/(R_o - R_i) = 130$) allows development of detectable disturbances for $\eta = 0.8$ and $Re \leq 320$. (Beyond $Re = 320$, the experimental Ta_{crit} values continue to grow with Re , while the computed values have essentially reached their plateau, as shown in table 2.)

Grosvenor (1981) and Greaves *et al.* (1983) used hot-wire anemometry to detect onset for $\mu = 0$ over essentially the same range ($43.75 \leq Re \leq 1112$) considered by Gravas & Martin (1978) for similar η . They reported Taylor numbers at four azimuthal positions in an annulus with less axial and azimuthal gap variation

(maximum 3.9% variation from the mean gap for $\eta=0.909$) than in that of Gravas & Martin. Each parenthetical Ta_{crit} in table 2 was taken from table A2 of Grosvenor (1981), and is the lowest value at the four positions. For $\eta=0.909$ (with aspect ratio ≈ 310), Ta_{crit}^{comp} at $Re=43.75$ lies less than 5% below Ta_{crit}^{expt} , with the discrepancy being about 9% at $Re=87.5, 131, \text{ and } 262$. The discrepancy decreases (to $\approx 6\%$) at $Re=435.5$, before Ta_{crit}^{expt} falls increasingly below Ta_{crit}^{comp} at higher Re . We interpret these results in terms of sufficient axial development length at low Re , with subcritical onset at higher Re . For $\eta=0.565$, computations at $Re=69.35, 198.9, \text{ and } 300.45$ show that computed values lie 40–54% below experimental values. This is consistent with a profoundly insufficient axial development length at an annular aspect ratio of less than 50.

For $\mu=0$ and $\eta=0.8$, Bühler & Polifke (1990) reported onset with $m_{crit}=1$ over $2.7 < Re < 4.6$, and with $m_{crit}=0$ at larger and smaller Re . They also reported a ‘scaloped’ $Re-Ta_{crit}$ stability boundary. Their results differ from ours at $\eta=0.77$ (figure 1a), and from specific computations for $\eta=0.8$, in which we find that instability sets in through an axisymmetric disturbance ($m_{crit}=0$) at $Re=3, 3.5, 4, \text{ and } 4.5$. The aspect ratio in the experiments of Bühler & Polifke was only 20.

Wave speeds

From the definition of the wave speed (see Part 1), one can show that $V_{drift}/\bar{V}_Z = c_{crit}$, where V_{drift} is the axial drift speed of the vortical structures. For $\mu=0$, our results can be compared to two previous reports of dimensionless axial drift speed. At Taylor numbers somewhat above critical, Donnelly & Fultz (1960) measured dimensionless drift speeds of 1.2₅, 1.0₇, and 1.3₆ at $Re=3.13, 4.40, \text{ and } 5.70$ for $\eta=0.949_7$, and Howes & Rudman (1998) obtained $V_{phase}/\bar{V}_Z = 1.16 \pm 0.005$ in slightly supercritical computations at $Re=2.61, Ta=12.5, \text{ and } \eta=0.9524$. These results compare very well to our computed c_{crit} values of 1.169 to 1.170 for $\eta=0.95$ over $0 \leq Re \leq 8$.

Figure 5 of Sorour & Coney shows experimental V_{drift}/\bar{V}_Z values at seven Re over $48 < Re \leq 500$ for $\eta=0.80$, and at 19 Re over $16 < Re < 610$ for $\eta=0.955$. For $\eta=0.80$, V_{drift}/\bar{V}_Z decreases monotonically from about 1.5 to about 0.3 over the experimental Re range. Computations for $\eta=0.77$ (see figure 1d) show that the computed c_{crit} decreases monotonically from 1.45 to 1.42 while $m_{crit}=2$ between $Re=38$ and 45, at which point c_{crit} jumps to 1.54, coincident with m_{crit} jumping to 3. At larger Re , the computed c_{crit} undergoes a series of jump increases, separated by progressively shorter Re intervals of monotonic decrease. On the scale of the experimental Re increments, however, c_{crit} increases monotonically. Computations for $\eta=0.8$ give similar results. For $\eta=0.955$, the experimental V_{drift}/\bar{V}_Z increases from about 1.6 near $Re=16$ to about 2.8 near $Re=100$, before decreasing to about 1.8 near $Re=610$. For $\eta=0.95$, c_{crit} is about 1.3 at $Re=10$, and for the experimental Re increments, increases monotonically and approaches an asymptote of about 3.3 just beyond the highest Re considered by Sorour & Coney. These results differ only slightly from those computed for $\eta=0.955$, and are in good agreement with the data. Simmers & Coney (1980) state that the earlier wave speed measurements of Sorour & Coney (for which Taylor numbers were not reported) were performed “with the flow just critical”, from which one can infer that over the Re range where the critical Ta values are in excellent agreement, the wave speed should be close to the critical values.

Figure 2 of the experimental paper by Wereley & Lueptow (1999) shows that for $\mu=0$ and $\eta=0.83$, m_{crit} jumps from 0 to 1 near $Re=8$. Our computations show that this jump occurs at $Re=16$ and 8 at $\eta=0.77$ and 0.95, respectively, suggesting that the

experimental Re for this change is slightly low. Also, invariance of Ta_{crit} with respect to the direction of the axial flow (see § 5.5 of Part 1) requires that dTa_{crit}/dRe vanish at $Re = 0$, suggesting a modification of the approximate boundary between SPF flow and propagating Taylor-like vortices shown in figure 2 of Wereley & Lueptow.

3.2. Comparison to experiments of Mavec and Snyder

Mavec (1973) and Snyder (1965) reported experimental results for a wide range of Re and μ at $\eta = 0.77$ and $\eta \approx 0.95$, respectively. To date, no comparison of their non-zero- μ data to computation or theory has been made. Here, we present computed values of Ta_{crit} for their combinations of $Re \neq 0$ and μ , along with a comparison to their data.

$$\eta = 0.77$$

For $\eta = 0.77$ and eleven Re in the range $24 \leq Re \leq 403.5$, Mavec reported critical combinations of $(N_{R\theta})_i = 2\Omega_i R_i (R_o - R_i)/\nu$ and $(N_{R\theta})_o = 2\Omega_o R_o (R_o - R_i)/\nu$, measured using aqueous glycerol solutions in an annulus with aspect ratio 160. For each Re , results were reported for a range of μ spanning negative and positive values.

We have read $(N_{R\theta})_i$ and $(N_{R\theta})_o$ values for each data point from Mavec's figure 4, and calculated $\mu = (N_{R\theta})_o \eta / (N_{R\theta})_i$ and the corresponding critical Taylor number, $Ta_{crit}^{expt} = (N_{R\theta})_i (1 - \eta) / 2\eta$. These, and Ta_{crit}^{comp} and m_{crit} at the calculated μ , are shown in table 3. Readability errors in $(N_{R\theta})_i$ and $(N_{R\theta})_o$ are small enough that calculated μ and Ta_{crit}^{expt} values are thought to be accurate to within 1%. For the 18 cases shown in table 3 for which $\mu > \eta^2 = 0.5929$, we expect that there is an Re range for which there are two values of Ta_{crit} , as discussed for $\mu = \eta = 0.5$ (see Part 1). For comparison to Mavec's results in these cases, we have computed only the smaller Ta_{crit} . In what follows, we consider the results in two Re ranges: $24 \leq Re \leq 106$, and $Re \geq 134.75$.

For each Re , the experimental and computed values of Ta_{crit} are unimodal functions of μ , providing that the two $\mu = 0$ data at $Re = 33, 49$, and 330 are averaged. At small Re , agreement between experimental and computed Ta_{crit} values is generally excellent. Over $24 \leq Re \leq 106$, there are 30 combinations of μ and Re for which experimental and computed results differ by less than 2%, including ten of the twelve μ values at $Re = 106$. This level of agreement suggests that the random errors in Mavec's experimental data are generally very small. Nonetheless, at small Re , there are still some systematic differences between experiment and computation. At each Re in $24 \leq Re \leq 106$, the experimental Ta_{crit} exceeds that predicted by linear theory if $\mu \leq -0.7$ or $\mu \geq 0.35$. For $-0.7 < \mu < 0.35$, we have calculated the mean and root-mean-square (r.m.s.) of the difference $\Delta = Ta_{crit}^{comp} - Ta_{crit}^{expt}$ between experimental and computed Ta_{crit} values, along with the variance of Δ , at each Re . For two Re , the mean and r.m.s. values are much larger than the variance. At $Re = 49$, the mean and r.m.s. differences are 3.3 and 3.4, respectively, and the variance is 0.45. (These values are not significantly reduced by averaging the two values at $\mu = 0$.) At $Re = 63.5$, the corresponding values are 3.1, 3.1, and 0.27. By contrast, the mean and r.m.s. differences and the variance are 0.25, 0.43, and 0.15, respectively, at $Re = 24$, and $-0.18, 0.41$, and 0.16 , respectively, at $Re = 106$. These results suggest small systematic errors in the experiments at $Re = 49$ and $Re = 63.5$, discussed below.

For $Re \geq 134.75$, the situation is quite different. First, in this range, the experimental and computational results agree within (the arbitrary) 2% at only eight points, four of which are at $Re = 134.75$, the smallest Re in this range. Second, in this range of

μ	Ta_{crit}^{expt}	Ta_{crit}^{comp}	m_{crit}^{comp}		μ	Ta_{crit}^{expt}	Ta_{crit}^{comp}	m_{crit}^{comp}
				<i>Re</i> = 24				
-0.37	33.64	33.70	1		0.33	39.58	39.97	0
-0.26	32.52	32.29	1		0.41	46.20	46.18	0
0	31.05	31.86	1		0.46	55.17	53.01	0
0.20	34.64	34.86	1		0.48	76.06	57.03	0
				<i>Re</i> = 33				
-0.52	38.58	39.10	2		0.17	36.93	38.65	1
-0.37	36.64	36.89	2		0.26	40.61	41.62	1
-0.19	35.22	35.67	2		0.43	55.64	55.07	1
0	33.61	35.97	1		0.50	75.12	70.82	1
0	34.58	35.97	1					
				<i>Re</i> = 49				
-1.01	54.73	54.10	4		0.11	42.81	46.36	4
-0.68	43.49	46.58	4		0.20	45.02	49.03	4
-0.36	40.81	43.14	4		0.25	46.93	51.12	5
-0.13	40.40	43.15	4		0.33	51.73	55.65	5
0	40.81	44.34	3		0.50	77.23	76.96	8
0	41.78	44.34	3					
				<i>Re</i> = 63.5				
-1.01	73.41	59.17	6		0	45.73	49.33	7
-0.94	55.38	55.13	6		0.17	48.99	52.62	8
-0.41	45.79	47.85	6		0.21	50.20	53.79	8
-0.26	44.76	47.60	6		0.24	51.49	54.80	9
-0.17	44.73	47.89	6		0.27	53.11	55.86	9
-0.10	45.37	48.29	7		0.52	77.23	74.13	11
				<i>Re</i> = 65.5				
-1.05	60.50	58.10	6		0.14	50.46	52.31	8
-0.48	48.26	48.77	6		0.19	51.64	53.59	9
-0.27	47.11	48.15	7		0.28	56.05	56.51	9
-0.20	47.37	48.26	7		0.39	62.82	61.88	10
-0.11	47.52	48.72	7		0.44	69.14	65.36	11
0	47.87	49.88	7		0.49	72.82	69.76	11
0.090	48.99	51.25	8					
				<i>Re</i> = 82.5				
-1.13	65.03	62.90	7		0	51.23	53.01	10
-0.58	51.88	53.31	8		0.13	52.70	54.58	11
-0.41	51.05	52.20	8		0.17	52.70	55.23	11
-0.30	51.05	51.86	9		0.21	54.58	56.00	11
-0.24	50.90	51.84	9		0.24	54.94	56.64	12
-0.13	50.61	52.17	10		0.44	63.85	62.65	13
-0.072	50.61	52.45	10		0.56	67.67	68.81	14
				<i>Re</i> = 106				
-0.93	65.03	62.18	9		0.095	56.11	55.91	13
-0.74	59.35	59.13	10		0.15	56.64	56.31	14
-0.51	56.88	56.70	11		0.24	56.94	57.02	14
-0.26	56.35	55.39	12		0.37	58.97	58.65	14
-0.14	55.17	55.23	12		0.59	64.85	63.33	15
0	55.20	55.47	13		0.81	78.79	77.32	15

μ	Ta_{crit}^{expt}	Ta_{crit}^{comp}	m_{crit}^{comp}	μ	Ta_{crit}^{expt}	Ta_{crit}^{comp}	m_{crit}^{comp}
$Re = 134.75$							
-0.78	70.47	63.36	12	0.56	57.88	58.99	16
-0.37	60.02	58.81	14	0.65	61.64	60.82	16
-0.26	59.29	58.04	14	0.87	70.03	75.10	15
-0.19	58.61	57.67	14	0.94	76.21	86.55	15
-0.054	57.52	57.09	15				
$Re = 166$							
-0.85	77.53	67.65	14	0.14	58.11	56.88	17
-0.67	69.14	64.79	15	0.23	57.97	56.49	17
-0.39	63.94	61.24	16	0.34	57.76	56.24	17
-0.23	63.11	59.60	16	0.48	56.79	56.49	17
-0.15	62.32	58.90	16	0.71	57.17	59.85	16
-0.083	60.52	58.38	16	0.84	67.70	66.67	15
0	60.41	57.75	17	0.96	69.59	80.01	15
0.091	58.29	57.15	17				
$Re = 244$							
-0.79	82.50	71.27	18	0.15	59.82	56.69	18
-0.70	74.65	69.52	18	0.29	57.88	55.50	18
-0.39	71.50	63.99	19	0.53	54.82	54.97	17
-0.25	66.94	61.78	19	0.77	54.73	59.02	16
-0.13	64.00	60.05	19	0.93	63.64	68.82	15
-0.058	63.05	59.09	19	1.01	67.82	77.81	14
0	62.38	58.36	19				
$Re = 330$							
-0.82	81.94	74.48	21	0.15	61.35	56.53	19
-0.67	79.29	71.05	21	0.27	57.67	55.32	19
-0.35	69.79	64.45	20	0.45	52.96	54.27	18
-0.18	67.29	61.35	20	0.67	50.17	55.48	17
-0.071	65.82	59.58	20	0.80	51.79	58.99	16
0	64.44	58.54	20	0.96	56.35	68.90	15
0	65.26	58.54	20	1.11	61.94	89.43	13
0.079	62.53	57.43	19				
$Re = 403.5$							
-0.63	79.65	71.05	22	0.20	60.17	55.87	19
-0.39	75.76	65.70	21	0.72	47.82	56.04	16
-0.29	71.29	63.67	21	0.84	48.85	60.30	16
-0.13	69.59	60.72	20	1.01	55.32	72.65	14
0	66.70	58.55	20	1.24	61.64	96.71	11
0.097	63.64	57.18	20				

TABLE 3. Comparison of computed values of Ta_{crit} to the experimental results of Mavec (1973) for $\eta = 0.77$.

larger Re , the difference Δ at each Re varies nearly monotonically with μ , beginning with $\Delta < 0$ for the most negative values of μ , and ending with $\Delta > 0$ for the most positive values. Linear least-squares fits of the form $\Delta = a\mu + b$ over $-0.7 < \mu < 0.35$ give values of the slope $a = 2.6, 3.1, 3.8, 4.3,$ and 4.7 at $Re = 134.75, 166, 244, 330,$ and 403.5 , respectively, compared to $0.67, 1.7, 1.4, 1.4, 1.3, 1.1,$ and 0.50 at $Re = 24, 33, 49, 63.5, 65.5, 82.5,$ and 106 , respectively. When all μ are included, the slopes are $-8.9, -2.5, 1.4, 6.1, -0.4, 1.2,$ and 0.2 at the lower Re values, and $6.6, 6.7, 9.2, 14.9,$ and 21.7 at the higher values.

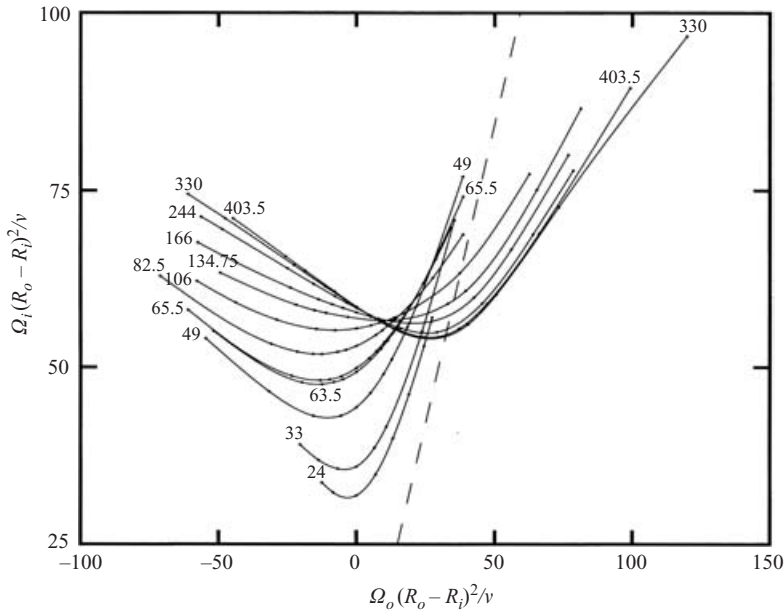


FIGURE 4. SPF stability boundaries for $\eta = 0.77$ and the values of Re (shown adjacent to each curve) and μ investigated experimentally by Mavec (1973). The dashed line corresponds to $\mu = \eta^2$.

The computed results presented in table 3 are shown in figure 4 using axes $\Omega_o(R_o - R_i)^2/\nu \equiv \mu Ta$ and $\Omega_i(R_o - R_i)^2/\nu \equiv Ta$, as is conventional for $Re = 0$ (cf. figure 6.2 of DiPrima & Swinney 1985). This representation is useful for assessing the effects of Re and understanding behaviour near the Rayleigh line ($\mu = \eta^2$). Figure 4 shows that for $\eta = 0.77$, the value of $\Omega_o(R_o - R_i)^2/\nu$ at which the critical $\Omega_i(R_o - R_i)^2/\nu$ attains its minimum initially shifts to more negative values as Re increases. At an Re apparently lying between 49 and 82.5, the location of this minimum shifts towards positive values of $\Omega_o(R_o - R_i)^2/\nu$, with the $\Omega_o(R_o - R_i)^2/\nu = 0$ axis being crossed between $Re = 106$ and 134.75. The high- Re plateau behaviour discussed in §§ 2.1–2.2 is reflected in the near-coincidence of the results for $Re = 330$ and 403.5. (Connection of the points in figure 4 by third-order splines is responsible for the slight apparent divergence of the curves for $Re = 330$ and 403.5 at sufficiently positive and negative μ .)

A number of Mavec's experimental points lie beyond the Rayleigh line ($\mu = \eta^2$). Thus, on the basis of results in Part 1, for some combinations of μ and Re we might expect two values of Ta_{crit} , depending on the location of the turning point (Re_{min}) for $\eta = 0.77$ and each μ considered. (With the axes used in figure 4, two values of Ta_{crit} correspond to a constant- μ straight line intersecting the stability boundary for a given Re at two different values of $\Omega_o(R_o - R_i)^2/\nu$.) For $Re = 106$ and $\mu = 0.81$, for which table 3 shows $Ta_{crit}^{expt} = 78.79$ and $Ta_{crit}^{comp} = 77.32$, we computed a second value, $Ta_{crit} = 463$. None of Mavec's results suggest that he encountered two critical values of Ω_o for a single μ , so in all other cases we have computed only the smaller Ta_{crit} for comparison to his results.

$\eta \approx 0.95$

For $\eta = 0.9497$ and 0.959 and seven non-zero Re up to 200, Snyder (1965) measured critical values of Ω_i for fixed values of Ω_o , for water in annuli with aspect ratios

between 285 and 349. The dimensionless results shown in his figures 1 and 2 ($\eta = 0.959$) and figure 3 ($\eta = 0.9497$) span a range of negative and positive μ for $0 \leq Re \leq 200$. For $Re > 0$, we have read $R_i^{1/2} \Omega_i (R_o - R_i)^{3/2} / \nu$ and $R_i^{1/2} \Omega_o (R_o - R_i)^{3/2} / \nu$ from these figures, and calculated the μ values shown in table 4 from the ratio. Values of Ta_{crit}^{expt} shown in table 4 were obtained by multiplying ordinates read from Snyder's figures by $[(1 - \eta)/\eta]^{1/2}$. Values of Ta_{crit}^{comp} and m_{crit} at each combination of Re , μ , and η are shown in table 4.

Agreement of our computations with the data of Snyder (1965) is generally excellent. In 43 out of 79 cases shown in table 4, the difference between Ta_{crit}^{comp} and Ta_{crit}^{expt} is less than 2.5%, the sum of Snyder's estimates of the systematic (1.5%) and statistical (1%) errors in his measurements of the critical angular velocity of the inner cylinder. For 34 combinations of Re and μ , Ta_{crit}^{comp} and Ta_{crit}^{expt} agree within 2%. In 20 cases, agreement is within 1%. These generally small differences between Ta_{crit}^{comp} and Ta_{crit}^{expt} imply that errors in the values of Ta and μ due to our reading of his figures 1–3 are also small. For $0 < Re \leq 40$, the mean and r.m.s. values of Δ (–0.41 and 0.43, –0.48 and 0.50, –0.64 and 0.78, and –0.08 and 0.26, for $Re = 5, 10, 20$, and 40, respectively) do not exceed 5% of Ta_{crit} . For $Re = 80$, agreement is within 2% for 13 of the 17 μ values. Even at the highest Re (200), agreement is within 2% at six of the 14 μ values.

As with the data of Mavec, there appear to be two types of systematic variation in Δ . First, at each Re , $|\Delta|$ is generally larger at the most positive and negative μ than at intermediate values. Second, there are Re values for which the variance of Δ is much smaller than its r.m.s. For example, for $Re = 5$ and 10, the variance of Δ , 0.017 and 0.021, respectively, is about 4% of the r.m.s. of Δ , strongly suggesting that the random contribution to the differences is very small compared to the already small r.m.s. differences. This suggests, at least for $Re = 5$ and 10, that differences between experiment and computation are largely systematic. As for Mavec's data, we have calculated linear least-squares fits $\Delta = a\mu + b$ to the differences as a function of μ for each Re . For $Re = 5, 10, 20, 40, 80, 120$, and 200, the calculated slopes are $a = -0.036, -0.033, -0.20, 0.31, -0.90, -0.95$, and -0.036 , respectively. (When only data in the range $-1.5 < \mu < 0.74$ are included, we find $a = -0.036, -0.033, 0.10, 0.31, 0.32, 0.95$, and 1.3 for the same Reynolds numbers.) The magnitudes of these slopes are considerably smaller than the corresponding slopes for the $\eta = 0.77$ data of Mavec.

Unlike the $\eta = 0.77$ case, table 4 shows that Ta_{crit}^{comp} significantly exceeds Ta_{crit}^{expt} for only a few combinations of Re and μ . Specifically, $\Delta/Ta_{crit}^{expt} > 0.04$ for $Re = 80$ at $\mu = -1.91$ ($\Delta/Ta_{crit}^{expt} = 0.08$), for $Re = 120$ at $\mu = 0.392$ ($\Delta/Ta_{crit}^{expt} = 0.18$), and for $Re = 200$ at $\mu = 0.146, 0.293$, and 0.417 ($\Delta/Ta_{crit}^{expt} = 0.05, 0.07$, and 0.07 , respectively). The relatively large, isolated discrepancy for $Re = 120$ at $\mu = 0.392$ has no obvious explanation. For $Re = 200$, Δ is quite small ($|\Delta| \leq 0.82$) for $\mu < 0$, increases monotonically to a maximum of 2.36 at $\mu = 0.417$, and falls rapidly to -5.16 at $\mu = 0.746$. This trend shows that the mechanisms of subcritical and delayed onset are unimportant for $\mu < 0$, with the latter becoming increasingly significant as μ increases beyond zero.

4. Discussion

4.1. Implications for interpretation of experiment

As shown in §§3.1 and 3.2, there is a broad range of Re and μ for which SPF loses its stability at Ta_{crit} values very close to those predicted by linear theory. Sometimes,

μ	Ta_{crit}^{expt}	Ta_{crit}^{comp}	m_{crit}^{comp}		μ	Ta_{crit}^{expt}	Ta_{crit}^{comp}	m_{crit}^{comp}
				<i>Re</i> = 5				
-0.738	12.19	11.78	3		0.238	9.628	9.169	0
-0.436	10.17	9.653	1		0.425	10.47	10.01	0
-0.243	9.436	9.026	0		0.668	13.45	12.94	0
0	8.936	8.809	0					
				<i>Re</i> = 10				
-0.731	12.30	11.78	3		0.234	9.790	9.416	1
-0.428	10.37	9.847	1		0.414	10.76	10.22	0
-0.234	9.794	9.243	1		0.656	13.70	13.05	0
0	9.263	9.053	1					
				<i>Re</i> = 20				
-0.924	16.21	15.33	5		0.204	12.08	11.56	1
-0.710	14.10	13.69	4		0.369	13.26	12.38	1
-0.393	12.48	11.86	2		0.620	15.99	15.61	1
-0.220	11.72	11.34	2		0.750	17.87	17.49	1
0	11.35	11.18	1		0.798	22.18	20.37	0
				<i>Re</i> = 40				
-1.06	16.78	16.30	9		0	14.74	14.79	3
-0.863	17.30	17.01	8		0.157	15.15	15.19	3
-0.631	15.86	15.88	7		0.299	16.28	15.95	2
-0.331	14.94	14.95	5		0.680	19.71	20.11	2
-0.168	14.84	14.73	4					
				<i>Re</i> = 80				
-1.91	23.46	25.50	18		0.117	20.99	20.84	29
-1.46	22.82	22.18	19		0.204	21.67	21.49	31
-1.09	20.40	20.33	20		0.383	23.28	23.45	36
-0.894	19.95	19.69	21		0.531	25.28	26.12	42
-0.687	19.48	19.28	22		0.628	28.65	28.85	48
-0.459	19.40	19.15	23		0.709	32.35	32.23	55
-0.233	19.55	19.40	25		0.823	40.88	40.79	69
-0.119	19.87	19.71	26		0.887	58.58	50.80	80
0	20.14	20.18	28					
				<i>Re</i> = 120				
-1.32	25.39	24.49	30		0.185	25.11	26.08	54
-0.932	24.00	23.39	33		0.392	23.26	28.47	63
-0.755	23.69	23.17	35		0.464	28.92	29.63	67
-0.565	23.63	23.15	38		0.573	31.34	31.90	73
-0.384	23.73	23.36	41		0.673	34.14	34.78	81
-0.195	24.00	23.85	44		0.801	42.06	40.44	92
-0.085	24.27	24.30	47		0.901	58.31	48.68	98
0	24.60	24.74	49					
				<i>Re</i> = 200				
-1.12	29.89	29.42	55		0	30.33	31.15	83
-0.748	29.89	29.17	62		0.146	30.53	32.08	89
-0.595	29.89	29.27	66		0.293	31.01	33.28	95
-0.448	29.79	29.50	69		0.417	32.19	34.55	101
-0.306	29.76	29.86	73		0.520	34.38	35.81	105
-0.150	30.06	30.42	78		0.603	37.71	37.00	109
-0.068	30.27	30.79	81		0.746	44.76	39.60	112

TABLE 4. Comparison of computed values of Ta_{crit} to the experimental results of Snyder (1965). Values in bold correspond to $\eta = 0.9497$; all other values are for $\eta = 0.9590$.

however, there are systematic differences. Here, we assess the contributions of the mechanisms of subcritical and delayed onset to these differences.

For the cases considered in §2, finite-amplitude instability corresponds to $Ta_{crit}^{expt} < Ta_{crit}^{comp}$. (For $\mu > \eta^2$, finite-amplitude onset on the upper branch of the stability boundary (see Part 1) would occur above the linear Ta_{crit} .) To date, little is known about nonlinear stability of SPF (Joseph & Munson 1970; Joseph 1976) or even non-rotating annular Poiseuille flow. For the latter, results are limited to a perturbation analysis for axisymmetric disturbances (Strumolo 1983), and to computational simulations at three Re (13 000, 15 500, and 20 000) at $\eta = 0.7$ with initial disturbances having one non-zero axial wavenumber (Shapiro, Shtilman & Tumin 1999). When axial flow between rotating cylinders is exactly a quadratic function of the radial coordinate (as can be arranged by choosing the relative axial velocity of the cylinders to exactly cancel the logarithmic term in (2.1c) of Part 1), Joseph & Munson (1970) have shown that finite-amplitude instability cannot occur for $\mu = 1$, and argued that this result should carry over approximately to $\mu \neq 1$. Based on what is known about finite-amplitude instability in related flows (e.g. circular Poiseuille flow), we conjecture that when finite-amplitude instability is possible in SPF at high Re , the amplitude threshold is sufficiently low for subcritical onset to be observed routinely.

For $\mu = 0$ and 0.2, Takeuchi & Jankowski (1981) found that their experimental Ta_{crit} values systematically exceeded predictions of linear analysis for Re greater than about 40. For $\mu = -0.5$, experimental Ta_{crit} values exceeded computed values for all $Re > 0$. They suggested that the linear stability analysis appears to be valid beyond the largest Re (100) at which they compared their computations and experiments. We note that Ta_{crit}^{expt} exceeding Ta_{crit}^{comp} cannot be regarded, by itself, as establishing the unimportance of finite-amplitude instability at a particular Re , since for the particular annular aspect ratio used, one of the mechanisms of onset delay might be the dominant effect, with finite-amplitude instability being observed only at larger aspect ratios. On the other hand, when Ta_{crit}^{expt} and Ta_{crit}^{comp} are nearly identical over a range of Re , the evidence for absence of finite-amplitude instability is much stronger.

For $\mu = 0$, comparison of the data of Kaye and co-workers to our computations shows that agreement is generally very good at small Re . As Re increases, Ta_{crit}^{expt} initially exceeds Ta_{crit}^{comp} . (One onset delay mechanism suggested by Takeuchi & Jankowski, involving a constant-head pump, is not applicable to the experiments of Kaye and co-workers, for which our results show that $dTa_{crit}/dRe \geq 0$ for $0 < Re < Re^*$.) As Re increases, Ta_{crit}^{expt} falls rapidly below the plateau value of Ta_{crit}^{comp} . It seems likely that, over some Re , there is competition between one or more of the mechanisms of subcritical and delayed onset. At sufficiently large Re , $Ta_{crit}^{expt} - Ta_{crit}^{comp}$ decreases and ultimately passes through zero. The results of Kaye & Elgar show that at sufficiently high Re , subcritical onset dominates, with onset occurring (at all Ta) at Re values close to those associated with finite-amplitude instability of plane and circular Poiseuille flow.

The reports of Kaye & Elgar and Yamada (1962) that Ta_{crit} falls to zero near $Re = 1000$ are consistent with known finite-amplitude instability in plane Poiseuille flow (corresponding to $\eta \rightarrow 1$ with no rotation) near $Re = 1000$ (Carlson, Widnall & Peeters 1982). Linear analysis would predict that $Re \rightarrow 5772$ (Orszag 1971) as $\eta \rightarrow 1$, consistent with monotonic decrease of the computed Re_{AP} values as $\eta \rightarrow 1$ (figure 5). The results of Kaye & Elgar, showing that $Ta_{crit} = 0$ near $Re = 1000$ for $\eta = 0.734$ and $Re = 900$ for $\eta = 0.820$, are consistent with Re values at which finite-amplitude instability is expected for annular Poiseuille flow. Extrapolation of the Ta_{crit}

values of Yamada (1961, 1962) to $Ta_{crit} = 0$ gives an Re value near 1200, much less than the $\eta \rightarrow 1$ plane Poiseuille non-rotating limit, and comparable to the value for finite-amplitude instability in that limit. This strongly suggests that finite-amplitude instability occurred in Yamada's experiments.

On the other hand, essentially perfect agreement between our computations and the data of Sorour & Coney for $\mu = 0$ and $\eta = 0.955$ in an annulus of high aspect ratio (> 570) up to $Re = 325$ convincingly shows that in their experiments the mechanisms of subcritical and delayed onset were unimportant. Since the disturbance level in their experiments, particularly at the entry to the rotating test section, seems to have been significant, the degree of agreement strongly suggests that either finite-amplitude instability does not occur for $Re \leq 325$, or if it does, the amplitude threshold is quite high or the range of subcritical Ta is very small. The degree of agreement between experiment and linear theory provides stronger evidence for the absence of finite-amplitude instability than any previously available for SPF, and quite likely for any shear flow.

For μ spanning a range of negative and positive values, agreement between the data of Snyder (1965) and Mavec (1973) and our computations is excellent over a wide range of Re and μ . However, even for small Re , there are values of Re and extreme values of μ for which systematic deviation occurs. Here, we discuss the implications of the agreement, as well as of the discrepancies, for interpretation of the experimental data.

Based on generally excellent agreement between Mavec's experiments and our computations at almost all 'intermediate' μ ($-0.70 < \mu < 0.35$) over $24 \leq Re \leq 106$, we conclude that subcritical and delayed onset mechanisms are unimportant in this regime.

For Mavec's data at $Re = 49$ and 63.5 , comparison of the mean and r.m.s. values of $\Delta = Ta_{crit}^{comp} - Ta_{crit}^{expt}$ to its variance strongly suggests the presence of small systematic errors, considerably larger than at other Re over $24 \leq Re \leq 106$. We conjecture, from the systematically positive Δ at those two Re and from the stability boundaries shown in figure 4, that the actual Re was somewhat lower than reported for these two cases.

For $Re \geq 134.75$, comparison of Mavec's data to our computations, and especially consideration of the slopes of $\Delta = a\mu + b$, suggests that as Re increases, mechanisms of onset delay become increasingly important except at the most positive μ , and that at these large rotation rate ratios, subcritical onset occurs at Ta_{crit} values lying progressively below the predictions of linear theory as μ and Re increase. Of the eight combinations of $Re \geq 134.75$ and μ for which experimental and computed Ta_{crit} values agree within 2%, four are at the lowest Re (134.75). At least two of the remaining four are at values of μ at which the experimental and computational results 'cross over', corresponding to a μ for which the competing effects of subcritical and delayed onset nearly cancel. This contrasts to the situation at $Re = 106$, for which experimental and computed Ta_{crit} values agree within 2% at nine consecutive μ .

Figure 5(a) shows a map of the experimental μ and Re considered by Mavec, with each symbol corresponding to our assignment of the nature of onset. We note that there is not a one-to-one correspondence between points for which either linear theory underpredicts the experimental Ta_{crit} ($\Delta < 0$) and those identified as 'delayed onset', or those for which $\Delta > 0$ and 'subcritical onset'. Rather, we have used Δ , its mean, variance, and r.m.s., and their dependence on Re and μ , to assign onset at each point. This assignment is somewhat subjective. For example, for $Re = 49$ and 63.5 , we characterize the transition as 'linear onset' over a broad range of μ ,

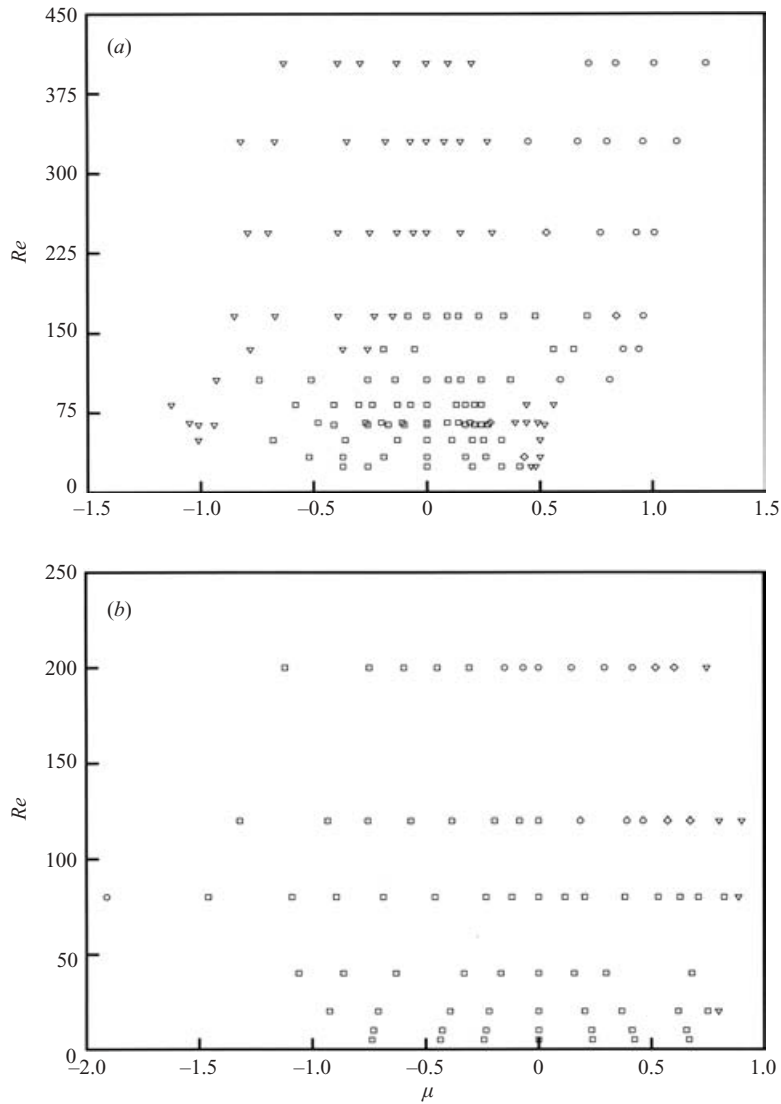


FIGURE 5. Nature of transition in (μ, Re) -plane for (a) $\eta = 0.77$ data of Mavec ($L/(R_o - R_i) = 160$) and (b) $\eta \approx 0.95$ data of Snyder ($285 \leq L/(R_o - R_i) \leq 349$): \square linear onset; \circ subcritical onset; ∇ delayed onset; \diamond competition between subcritical and delayed onset.

since the small variance of Δ compared to its mean and r.m.s. values suggests that consistently positive Δ are associated with small errors in Re rather than subcritical onset. For several Re , it appears (as discussed above) that subcritical onset and onset delay compete with each other, giving Δ values of opposite sign at consecutive μ , with magnitudes considerably greater than the low variance of Δ in the low and intermediate range of $|\mu|$. These points, which we characterize as ‘competing’, include several of the high- Re points at which isolated small values of Δ were found.

There is a broad range of Re and μ in which subcritical onset is not apparent in the experiments of Mavec. The onset map suggests that finite-amplitude instability was

not observed for $Re < 106$, and at higher Re occurred only at sufficiently positive μ , with the required μ decreasing with Re . On the other hand, onset is delayed at large μ even for small Re . At larger Re , competition between the mechanisms of subcritical and delayed onset seems to occur at rotation rate ratios intermediate between large μ at which onset is subcritical and smaller μ at which linear theory accurately predicts onset. For $Re \geq 244$, our map suggests that linear onset was not observed in Mavec's experiments, being subcritical for sufficiently positive μ , and delayed for smaller μ . In general, increasing μ at fixed Re leads to a transition from delayed to linear onset, to competition between the mechanisms of subcritical and delayed onset, and finally to subcritical onset.

In Snyder's experiments with $\eta \approx 0.95$, the extremely small variance of Δ for some Re suggests that differences between computed and experimental Ta_{crit} values are largely due to small systematic errors. In particular, we note the 4% variance of the already small r.m.s. values of Δ for $Re = 5$ and 10. As for similar cases in Mavec's data, we conjecture that this is associated with a (small) difference between the reported and actual Re , as discussed above for Mavec's data at $Re = 49$ and 63.5, with the sign ($\Delta < 0$) indicating that the actual Re was larger than reported in these cases.

The generally smaller slopes of the least-squares lines $\Delta = a\mu + b$ for Snyder's data compared to Mavec's data suggest that subcritical instability and onset-delaying mechanisms were less important in Snyder's experiments, in which the radius ratio was larger than Mavec's, as was the annular aspect ratio.

Figure 5(b) shows an onset map for the experiments of Snyder (1965). Compared to results shown in figure 5(a), the most dramatic difference is the wider range of Re and μ over which subcritical instability does not occur. The map indicates that subcritical instability was not observed in Snyder's experiments for $Re < 120$, except at one point ($Re = 80$, $\mu = -1.91$), where μ assumes its most negative value in the experiments of Mavec or Snyder. For larger Re , subcritical effects appear to be manifested in a μ range whose width increases with increasing Re . With the exception of the $Re = 80$, $\mu = -1.91$ point, increasing μ at fixed Re leads to a change from linear to subcritical onset (when Re is high enough), to competition between the mechanisms of subcritical and delayed onset, and ultimately to significant delay of onset.

Figures 5(a) and 5(b) show a broad qualitative similarity in the regions of the (μ, Re) -plane in which linear onset of instability in SPF occurred in the experiments of Mavec and Snyder. In both cases, onset is closely predicted by linear theory up to at least $Re = 166$ (200 for Snyder's experiments) over a significant range of μ . For Mavec's $\eta = 0.77$ experiments with $L/(R_o - R_i) = 160$, we judge onset at $Re = 166$ to occur by a linear mechanism for $-0.083 \leq \mu \leq 0.84$. For Snyder's experiments with $\eta \approx 0.95$ and $285 \leq L/(R_o - R_i) \leq 349$, we judge onset to occur by a linear mechanism at the highest Re (200) for $-1.32 \leq \mu \leq 0.464$ (i.e. at all but the three largest μ values). At smaller Re , onset appears to be linear for a somewhat wider range of negative μ in Snyder's experiments than in Mavec's. In Mavec's experiments, subcritical instability occurs over a progressively broader range of positive μ as Re increases, while in Snyder's, with larger radius ratio and aspect ratios, departures from linear onset at positive μ are associated with delayed onset.

If, to a first approximation, we associate delayed onset with finite aspect ratio effects, and subcritical onset with the nominal base flow (depending on Re , μ , and η), then we might conjecture that subcritical onset is less important (e.g. occurs over a smaller range of Re and μ , or has a higher amplitude threshold, or occurs over a narrower range of Ta lying below the Ta_{crit} of linear theory) in the higher- η experiments of Snyder.

4.2. Relationship to annular Poiseuille flow

As discussed in Part 1, connection of the low- Re Taylor–Couette instability to the high- Re instability of annular Poiseuille flow had been made prior to the present work only for $\mu=0$ and $\eta=0.95$, subject to the limitation of axisymmetric disturbances (Ng & Turner 1982). As shown in §2.2, transition for $\mu=0$ and $\eta=0.95$ actually occurs from non-axisymmetric centrifugal instability to non-axisymmetric Tollmien–Schlichting-like instability. As for $\eta=0.5$, transition from centrifugal instability to the TS-like instability occurs just below $Re = Re_{AP}$ for each combination of μ and η considered.

For each combination of μ and η , m_{crit} decreases from its value on the high- Re plateau to 2 as one passes through Re^* . Beyond Re^* , m_{crit} is non-increasing, and at Re_{AP} assumes the values of 1 and 0 for $\eta=0.77$, and 0.95, respectively. The non-zero m_{crit} at Re_{AP} for $\eta=0.77$ is at variance with the expectation that the critical disturbance is axisymmetric as Re approaches Re_{AP} (Ng & Turner 1982, p. 101).

4.3. Relationship to the narrow-gap limit

For $\mu=0$, we note that the initial range, $0 \leq Re \leq Re_0$, for which $m_{crit}=0$, is progressively reduced as $\eta \rightarrow 1$, with $Re_0=24$, 16, and 8 for $\eta=0.5$, 0.77, and 0.95, respectively. This suggests that in the narrow-gap limit, the initial range of Re for which instability sets in as axisymmetric Taylor-like vortices propagating downstream will be small. The only prior theoretical work accounting for non-axisymmetric disturbances for $\mu \neq 0$ in the narrow-gap limit is that of Chung & Astill (1977), errors in which have been discussed by Takeuchi & Jankowski and Ng & Turner.

The only experimental work for $\mu \neq 0$ in the narrow-gap limit is that of Snyder (1965), for $\eta \approx 0.95$ over the ranges $0 \leq Re \leq 200$ and $-2 \leq \mu \leq 0.92$, with the upper bound on μ being approximately the value beyond which circular Couette flow is linearly stable (Synge 1938). For $\mu=0.2$, it is evident from points near the $\mu=0.2$ line in Snyder's figure 1 that Ta_{crit} increases monotonically with Re over the range investigated. This is consistent with the trend suggested by our results for $\eta=0.5$ (Part 1) and 0.77 (figure 2a), where we see that as η increases, (a) there is an increase in the Re beyond which axial shear destabilizes SPF with respect to centrifugal instability, (b) the magnitude of that destabilization decreases, and (c) the plateau begins at higher Re . Together with our results for $\eta=0.5$ and 0.77, the results of Snyder suggest that at least for $\mu=0.2$, axial flow does not reduce the critical Ta for onset of centrifugal instability in the limit $\eta \rightarrow 1$.

For the Taylor number definition used by Takeuchi & Jankowski and in the present work, Ta_{crit} vanishes for $Re=0$ as $\eta \rightarrow 1$. Figure 6 shows the $\mu=0$ results of §2 plotted in terms of a modified Taylor number defined by

$$\hat{T}a = Ta \left(\frac{\eta}{1-\eta} \right)^{1/2}, \quad (4.1)$$

the critical value of which approaches $\sqrt{1707.762 \dots}$ as $\eta \rightarrow 1$ for $Re=0$ and $\mu=0$. It appears that the plateau value of $\hat{T}a$ grows without bound as $\eta \rightarrow 1$. Note that Re_{AP} approaches the plane Poiseuille limit $Re=5772$ from above as $\eta \rightarrow 1$. Finally, we note that $m_{crit}=0$ at Re_{AP} for $\eta=0.95$ is consistent with the expected behaviour as $\eta \rightarrow 1$, based on the two-dimensionality of the critical TS disturbance in plane Poiseuille flow.

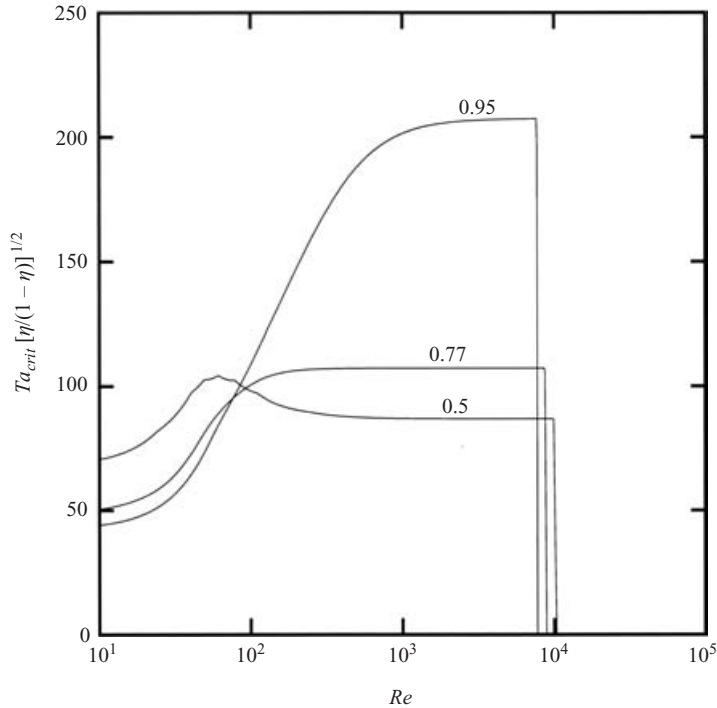


FIGURE 6. Critical $Ta[\eta/(1-\eta)]^{1/2}$ versus Re for $\mu=0$ and $\eta=0.5, 0.77$, and 0.95 .

5. Conclusions

The complete linear stability boundaries for spiral Poiseuille flow show that for $\eta=0.77$ and 0.95 and each rotation rate ratio $\mu < \eta^2$ considered, we can connect the onset of instability for circular Couette flow to the onset of instability in annular Poiseuille flow. For $\mu > \eta^2$, no instability is possible on a linear basis from $Re=0$ up to a turning point beyond which the stability boundary is multi-valued and SPF is stable in two disjoint Ta ranges. For $\mu < \eta^2$, an axial pressure gradient stabilizes SPF with respect to centrifugal instability up to high Re , as shown by Ng & Turner. In each case, Ta_{crit} reaches a plateau before falling precipitously to zero as Re approaches Re_{AP} , the critical Re for annular Poiseuille flow. The transition from centrifugal instability at small Re to a shear instability of Tollmien–Schlichting type occurs at Re^* (slightly smaller than Re_{AP}), at which the critical azimuthal wavenumber drops from its value on the high- Re plateau to $m_{crit}=2$ in each case considered.

Comparison to data for $\mu=0$ shows that for each η and aspect ratio, there is an Re range in which subcritical instability does not occur, and for which the annulus is long enough to allow development of detectable secondary flow. For a narrow-gap ($\eta=0.955$) annulus of large aspect ratio (> 570), agreement between experiment and computation is essentially exact up to $Re=325$, showing that neither finite-amplitude instability nor any other type of subcritical onset occurs over a wide range of Re when the outer cylinder is fixed. For $\eta=0.77$ and $\eta \approx 0.95$, comparison to data up to $Re > 100$ suggests existence of a substantial range of μ and Re in which subcritical onset does not occur.

The authors thank Drs John E. R. Coney and Roger I. Grosvenor and Professor Howard A. Snyder for providing access to their original data, Professor Hassan M. Nagib for providing a copy of the thesis of Mavec, and Professor Snyder and anonymous reviewers for helpful comments. This work was supported in part by NSF Grants CTS-9422770 and CTS-9613241, and DOE Grant DE-FG02-96ER45607. Some of the computations were performed using the facilities of the National Center for Supercomputing Applications.

REFERENCES

- BECKER, K. M. & KAYE, J. 1962 Measurements of diabatic flow in an annulus with an inner rotating cylinder. *J. Heat Transfer* **84**, 97–105.
- BÜHLER, K. & POLIFKE, N. 1990 Dynamical behaviour of Taylor vortices with superimposed axial flow. In *Nonlinear Evolution of Spatio-Temporal Structures in Dissipative Continuous Systems* (ed. F. H. Busse & L. Kramer), pp. 21–29. Plenum.
- CARLSON, D. R., WIDNALL, S. E. & PEETERS, M. F. 1982 A flow-visualization study of transition in plane Poiseuille flow. *J. Fluid Mech.* **121**, 487–505.
- CHUNG, K. C. & ASTILL, K. N. 1977 Hydrodynamic instability of viscous flow between coaxial cylinders with fully developed axial flow. *J. Fluid Mech.* **81**, 641–655.
- COTRELL, D. L. & PEARLSTEIN, A. J. 2004 The connection between centrifugal instability and Tollmien–Schlichting-like instability for spiral Poiseuille flow. *J. Fluid Mech.* **509**, 331–351 (referred to herein as Part 1).
- DIPRIMA, R. C. & SWINNEY, H. L. 1985 Instabilities and transition in flow between concentric rotating cylinders. In *Hydrodynamic Instabilities and the Transition to Turbulence* (ed. H. L. Swinney & J. P. Gollub), 2nd edn, pp. 139–180. Springer.
- DONNELLY, R. J. & FULTZ, D. 1960 Experiments on the stability of viscous flow between rotating cylinders. II. Visual observations. *Proc. R. Soc. Lond. A* **258**, 101–123.
- GARG, V. K. 1980 Spatial stability of concentric annular flow. *J. Phys. Soc. Japan* **49**, 1577–1583.
- GRAVAS, N. & MARTIN, B. W. 1978 Instability of viscous axial flow in annuli having a rotating inner cylinder. *J. Fluid Mech.* **86**, 385–394.
- GREAVES, P. L., GROSVENOR, R. I. & MARTIN, B. W. 1983 Factors affecting the stability of viscous axial flow in annuli with a rotating inner cylinder. *Intl J. Heat Fluid Flow* **4**, 187–197.
- GROSVENOR, R. I. 1981 Axisymmetry of spiral Taylor vortex flow in annuli and the effect of gap width variations. M.Eng. Thesis, Univ. Wales Inst. Sci. Tech., Cardiff.
- HOWES, T. & RUDMAN, M. 1998 Flow and axial dispersion simulation for traveling axisymmetric Taylor vortices. *AIChE J.* **44**, 255–262.
- JOSEPH, D. D. 1976 *Stability of Fluid Motions I*. Springer.
- JOSEPH, D. D. & MUNSON, B. R. 1970 Global stability of spiral flow. *J. Fluid Mech.* **43**, 545–575.
- KAYE, J. & ELGAR, J. 1958 Modes of adiabatic and diabatic fluid flow in an annulus with an inner rotating cylinder. *Trans. ASME* **80**, 753–765.
- MAHADEVAN, R. & LILLEY, G. M. 1977 The stability of axial flow between concentric cylinders to asymmetric disturbances. *AGARD CP-224*, pp. 9-1–9-10.
- MAVEC, J. A. 1973 Spiral and toroidal secondary motions in swirling flows through an annulus at low Reynolds numbers. MS Thesis, Illinois Inst. Tech., Chicago.
- MESEGUER, A. & MARQUES, F. 2002 On the competition between centrifugal and shear instability in spiral Poiseuille flow. *J. Fluid Mech.* **455**, 129–148.
- NAGIB, H. M. 1972 On instabilities and secondary motions in swirling flows through annuli. PhD Dissertation, Illinois Inst. Tech., Chicago.
- NG, B. S. & TURNER, E. R. 1982 On the linear stability of spiral flow between rotating cylinders. *Proc. R. Soc. Lond. A* **382**, 83–102.
- ORSZAG, S. A. 1971 Accurate solution of the Orr–Sommerfeld stability equation. *J. Fluid Mech.* **50**, 689–703.
- SHAPIRO, I., SHTILMAN, L. & TUMIN, A. 1999 On stability of flow in an annular channel. *Phys. Fluids* **11**, 2984–2992.

- SIMMERS, D. A. & CONEY, J. E. R. 1980 Velocity distributions in Taylor vortex flow with imposed laminar axial flow and isothermal surface heat transfer. *Intl J. Heat Fluid Flow* **2**, 85–91.
- SNYDER, H. A. 1962 Experiments on the stability of spiral flow at low axial Reynolds numbers. *Proc. R. Soc. Lond. A* **265**, 198–214.
- SNYDER, H. A. 1965 Experiments on the stability of two types of spiral flow. *Ann. Phys.* **31**, 292–313.
- SOROUR, M. M. 1977 Hydrodynamic stability, with special reference to the effect of heat transfer, in a concentric annulus having an inner rotating wall. PhD Thesis, Leeds University.
- SOROUR, M. M. & CONEY, J. E. R. 1979 An experimental investigation of the stability of spiral vortex flow. *J. Mech. Engng Sci.* **21**, 397–402.
- STRUMOLO, G. S. 1983 Perturbed bifurcation theory for Poiseuille annular flow. *J. Fluid Mech.* **130**, 59–72.
- SYNGE, J. L. 1938 On the stability of a viscous liquid between two rotating coaxial cylinders. *Proc. R. Soc. Lond. A* **167**, 250–256.
- TAKEUCHI, D. I. & JANKOWSKI, D. F. 1981 A numerical and experimental investigation of the stability of spiral Poiseuille flow. *J. Fluid Mech.* **102**, 101–126. Corrigendum **113**, 536 (1981).
- WERELEY, S. T. & LUEPTOW, R. M. 1999 Velocity field for Taylor–Couette flow with an axial flow. *Phys. Fluids* **11**, 3637–3649.
- YAMADA, Y. 1961 Torque and pressure drop of the flow between rotating co-axial cylinders in low Reynolds number. *Trans. JSME* **27**, 610–618. (Title and Abstract in English.)
- YAMADA, Y. 1962 Resistance of a flow through an annulus with an inner rotating cylinder. *Bull. JSME* **5**, 302–310.